DOI:
10.1002/uog.27609

Document Version
Peer reviewed version

Bartin Raphael (Orcid ID: 0000-0001-8675-0846)
Salomon Laurent J (Orcid ID: 0000-0003-0627-4347)

Static and dynamic responses to hyperoxia of normal placenta across gestation with T2*-weighted sequences

R. Bartin[1,2], A. Melbourne[3,4], L. Bobet[2], G. Gauchard [2], A. Menneglier[2], D. Grevent[2,5], L. Bussieres[1,2], N. Siauve[6], L. J. Salomon[1,2]

[1]Department of fetal medicine, surgery and imaging, Hôpital universitaire Necker enfants malades, AP-HP, Paris, France

[2]Plateforme LUMIERE, Hôpital universitaire Necker enfants malades, URP 7328 and PACT, affiliated to Imagine Institut, Université de Paris, Faculté de médecine, Paris, France

[3]Department of Medical Physics and Biomedical Engineering, University College London, London, UK

[4]School of Biomedical Engineering & Imaging Sciences, Kings College London, London, UK

[5]Department of pediatric radiology, Hôpital universitaire Necker enfants malades, AP-HP, Paris, France

[6]Department of radiology, Hôpital Louis Mourier, AP-HP, Colombes, France

Correspondence:

Prof. L. J. Salomon, Hôpital universitaire Necker enfants malades, 149 rue de Sèvres, 75015, Paris, France.

(e-mail: laurentsalomon@gmail.com)

Running Head: Placental uptake and transfer of oxygen using MRI.

Keywords: Placental function, fetal MRI, T2*-weighted sequences, BOLD MRI

CONTRIBUTION

What are the novel findings of this work?

Our BOLD protocol was consistent with a free-diffusion model of oxygenation, illustrating to the growing difference in oxygen saturation between mother and fetus across gestation ($\Delta BOLD$), and changes in placental permeability to oxygen (λ).

What are the clinical implications of this work?

In a cohort of 52 uncomplicated pregnancies, both placental T2* histogram analysis and BOLD dynamic parameters suggest that the reduction in apparent oxygenation over gestation in baseline conditions, assessed by T2* relaxometry, does not reflect a loss in placental ability to uptake and transfer oxygen.

ABSTRACT

OBJECTIVES: T2*-weighted sequences have been identified as non-invasive tools to study the placental oxygenation in-vivo. This study aims to investigate both static and dynamic responses to hyperoxia of the normal placenta across gestation.

METHODS: We conducted a single-center prospective study including 52 uncomplicated pregnancies. Two T2*-weighted sequences were performed: T2*-relaxometry was performed before and after maternal hyperoxia. The histogram distribution of T2* values was assessed by fitting a gamma distribution as $T2* \sim \Gamma(\alpha, \beta)$. A dynamic acquisition (BOLD protocol) was also performed before and during oxygen supply, until placental oxygen saturation. The signal change over time was modeled using a sigmoid function, used to determine the intensity of enhancement ($\Delta BOLD, \%$), a temporal variation coefficient (λ, min^{-1}, controlling the slope of the curve), and the maximal steepness (Vmax, $\Delta BOLD.min^{-1}$) of placental enhancement.

RESULTS: The histogram analysis of the T2* values in normoxia showed a whole-placenta variation, with a decreasing linear trend in the mean T2* value (R= -0.83, 95% CI [-0.9, -0.71], p<0.001) along with a more peaked and narrower distribution of T2* values across gestation. After maternal hyperoxia, the mean T2* ratios (mean $T2*_{hyperoxia}$/ mean $T2*_{baseline}$) were positively correlated with gestational age, while the other histogram parameters remained stable, suggesting a translation of the histogram towards higher values with a similar aspect. The $\Delta BOLD$ showed a non-linear increase across gestation. Conversely, the λ (min^{-1}) parameter, showed an inverted trend across gestation, with a significantly weaker correlation (R = -0.33, 95% CI [-0.58, -0.02], p=0.04, R^2 = 0.1). As a combination of $\Delta BOLD$ and λ, the changes in Vmax throughout gestation were mainly influenced by the changes in $\Delta BOLD$ and resulted in a positive non-linear correlation with gestational age.

CONCLUSION: Our results suggest that the decrease in the T2* placental signal over gestation does not reflect a dysfunction. The BOLD effect, representative of a free-diffusion model of oxygenation,

highlights the growing differences in oxygen saturation between mother and fetus across gestation ($\Delta BOLD$), and placental permeability to oxygen (λ).

INTRODUCTION

The placenta is a temporary but yet major organ of pregnancy. It constitutes the main interface between mother and fetus and develops across gestation to adapt to its growing needs. Among all the roles carried out by the placenta, oxygen supply is a key mechanism to ensure adequate growth and fetal development. Through passive diffusion, oxygen transfers from the surrounding maternal compartment (intervillous space) into the fetal villous trees, facilitated by the difference in oxygen concentration between both compartments (intervillous PO_2 > fetal-villous PO_2) and the difference in hemoglobin oxygen affinity between adult and fetal hemoglobin.[1] Hence, placental insufficiency reduces the transfer of oxygen leading to complications such as intrauterine growth restriction (IUGR).[2] Fetus with IUGR remain below their theoretical growth potential and are at higher risk for perinatal morbidity and mortality,[3] and poor long-term outcomes.[4–6] Routine evaluation of placental function and fetal growth currently relies on repeated ultrasound weight estimation and Doppler measurements throughout the pregnancy.[7–10] However, Doppler patterns may remain stable despite an altered placental function and predicting the following evolution of a small fetus is challenging. [11,12] Thus, there is an important need for new methods to assess placental function.

In-vivo assessment of placental oxygenation may be achieved by using magnetic resonance imaging (MRI), particularly through T2*-weighted sequences.[13–15] Due to their intrinsic characteristics, T2*-weighted sequences are sensitive to magnetic field inhomogeneities and thus, to local variations in hemoglobin saturation.[16] These emerging methods may have the potential to identify placental dysfunction with a higher accuracy than ultrasound and Doppler follow-up.[17–20] While T2* parametric maps may be used to indirectly quantify placental apparent oxygenation and aging,[13,21–23] blood-oxygen level dependent (BOLD) effect quantifies the placental response to a variation of the baseline oxygen conditions.[24,25] Both acquisition methods provide complementary information and could be combined to describe more precisely the placental function and its change across gestation.

Thus, we aim to characterize the response of the normal placenta to maternal hyperoxia and to define objective and quantitative dynamic parameters to describe the dynamics of placental oxygen uptake across gestation.

METHODS

Study population

Patients were recruited prospectively between February 15th to July 30th 2022, as part of the ongoing project (ClinicalTrials.gov, NCT04142606). All patients gave written and informed consent. We included singleton uncomplicated pregnancies from 16 to 36 weeks of gestation, defined as the absence of obstetrical complication including pre-eclampsia, gestational hypertension, low estimated fetal weight (<10th centile) or fetal anomaly prior to MRI scan. To ensure their status of uncomplicated pregnancy, following MRI scans, complete pregnancy and neonatal outcomes were collected. An ultrasound was performed the same day as the MRI scan for all patients. Measurements included fetal weight estimation, maternal and fetal Doppler patterns.

MRI acquisitions and analysis

Placental MRI scans were performed with a 1.5 Tesla wide-bore 70 cm system, GE Optima™ MR450w (GE Healthcare, Milwaukee, WI). Patients were placed in supine position and an eight-channel cardiac coil was placed over the abdomen, covering the entire pelvic area. After anatomical sequences performed to localize the placenta, T2* relaxometry was performed under normoxia (baseline conditions). This was followed by a dynamic BOLD acquisition, in which the first 3 minutes were acquired under normoxia and were followed by a period of oxygen supply (7 to 9 minutes) through a non-rebreather facial mask (15L/min), maintained until the end of the whole protocol. Finally, a second T2* relaxometry was performed under hyperoxia. The general MRI protocol is summarized in Figure 1A, and parameters from both sequences in Table 1.

The protocol was performed under constant clinical supervision. In case of poor clinical tolerance, the acquisition was stopped, resulting in the exclusion of the patient from the BOLD analysis.

Placental T2* mapping

T2* parametric maps were generated from a multi-echo gradient-echo sequence with the following parameters: repetition time, 92.7 ms; 16 echoes times ranging from 3.0 to 77.3 ms in steps of 4.96 ms; field of view, 360 × 360 mm, slice thickness of 7 mm. Two to four slices were obtained in an axial orientation. Each slice was acquired within a single breath-hold of 12 s.

T2* maps were computed by fitting a voxel-wise mono-exponential decay model. Placental T2* values were then extracted and merged into a single histogram. Because the distribution of observed T2* values was positive and positively skewed, we fitted a gamma distribution by maximum likelihood, as $T2* \sim \Gamma(\alpha, \beta)$, describing the structure of the histogram using the mean T2* value, the shape parameter (α) and the rate (β). Lower values of α result in a more peaked and less skewed distribution. The rate parameter (β) describes the spread of the distribution. Lower values of β widen the distribution. These parameters are related by $mean = \alpha/\beta$. The procedure was performed under normoxia and repeated after hyperoxia (Figure 1B). Ratios of histogram parameters (hyperoxia to maternal-normoxia values) were used to compare histogram aspects before and after oxygen supply. Examples of T2* mapping, along with their corresponding histograms and gamma distribution are displayed in the supplementary material (Figure S1).

BOLD protocol and dynamic parameters

Following the first T2* relaxometry, a dynamic acquisition was performed using a gradient-echo echo-planar imaging sequence with the following parameters: repetition time = 8000 msec, echo time = 50 msec, flip angle = 90°, Field-of-view of 360x360 mm.

The mean placental signal-over-time curves were obtained by using an in-house Python script. Our protocol resulted in a 3-phase signal change: a first 3-minute steady state (baseline acquisition under normoxia) was followed by a second phase of enhancement during oxygen supply and ended-up in a new steady-state after reaching a new equilibrium. After exclusion of the first two timepoints, the overall signal was normalized to the baseline signal, and a sigmoid function was fitted to the data using a non-linear least square regression, modelled by the following equation:

$$Snorm(t) = \frac{S(t)}{Sbaseline} = \frac{\Delta BOLD}{1 + e^{-\lambda(t-\mathrm{t1/2})}} + 1 \ (eq.1)$$

Where:

- $Sbaseline$ was estimated using the mean signal from timepoints 3 to 16
- $\Delta BOLD$ (%) describes the percentage of placental enhancement.
- λ (min^{-1}) represents the steepness or slope of the curve, and basically controls how quickly the curve transitions from its minimum to its maximum value.
- $t_{1/2}$ corresponds to the inflexion point (or time to reach half of the maximum signal).

Finally, to compare the rate of signal increase (or steepness) during oxygen supply between patients, which is not constant but varies along the sigmoid curve, we decided to report the maximal steepness that occurs at the inflexion point: $V_{max} = \frac{dSnorm(t)}{dt}\,[t_{1/2}] = \frac{\lambda \Delta BOLD}{4}$ *(% of enhancement.min^{-1})*$(eq.2)$. Data and fitted curves are illustrated in Figure 1C and 1D.

Placental segmentation

Masks were drawn manually on a single timepoint to cover a large placental area (8 to 15 slices, depending on the gestational age). To avoid non-placental tissue in the manual segmentation due to maternal breathing, fetal motion and potential contractions within the 10-12 minutes of dynamic acquisition, the masks were cropped on the edges, hence containing the largest area common to all timepoints.

Statistical analysis

Histogram parameters

The changes in histogram parameters at baseline and after maternal hyperoxia across gestation were estimated using ordinary linear regressions. Correlations were assessed by the Pearson product-moment correlation.

BOLD protocol and dynamic acquisition

To model the change in BOLD parameters across gestation, different methods were tested, including linear, polynomial, and cubic spline polynomial regressions. Assessment of goodness of fit relied on

inspection of residuals with quantile-quantile plots, and residuals vs fitted plots. In two cases, artifacts during acquisition resulted in fitting imprecision in both λ and $Vmax$: those cases were identified as outliers and excluded from the final analysis. Details of our method for detection of outliers, along with the results of the models with and without outliers are presented in supplemental material (Appendix S1, Tables S1 and S2, Figures S2 and S3). All statistical analysis were carried out in R *(http://www.r- project.org; R Foundation, Vienna, Austria).*

RESULTS

Study population

Characteristics of the 52 patients are summarized in table 2. Patients were included from 16 to 36 weeks of gestation, with a median gestational age at MRI of 26.9 weeks, IQR (23.6, 32.1). The first trimester estimation of pre-eclampsia risk was available for 41/52 patients of our cohort who underwent their first trimester screening at our institution, with a median risk of 1/548, IQR (1/1368, 1/230). For 5 patients, despite having no previous medical history of pre-eclampsia or hypertension, risk estimation was > 1/100 and Aspirin was prescribed. All five patients had uncomplicated pregnancy and delivery. Ultrasound measurements, performed the same day as the MRI scan, confirmed normal fetal weight estimation and normal Doppler patterns. Only one patient presented with bilateral uterine notch at 23.4 weeks of gestation.

Changes in T2* histogram parameters throughout gestation

T2 histogram parameters at baseline*

Changes in T2* histogram parameters across gestation in standard conditions (baseline state) are presented in Figure 2. The placental mean T2* signal (Fig. 2A) significantly correlated to the gestational age and dropped by 4.15 ms per week, following a linear decrease as 221.80 ms-4.15 ms/week (Pearson correlation coefficient R= -0.83, 95% CI [-0.9, -0.71], R^2=0.69, p<0.001). The aspect of the histogram was assessed by the α and β parameters of a gamma distribution. The α parameter followed a similar linear decrease across gestation of 23.6-0.42/week, (Pearson correlation coefficient R = - 0.64, 95% CI [-0.79, -0.43], p<0.001, Figure 2C). The β parameter, however, seemed unrelated to the gestational age, with a mean rate of 0.12+/-0.03 (fig. 2D). Hence, with a fixed β, the overall aspect of the histogram only depended on the α-parameter. Altogether, the T2* values decreased with advancing gestational age with a narrower distribution (increasing homogeneity), and an increasing

skewness (right-tailed extension). The simulated changes in T2* placental histogram throughout gestation are illustrated in Figure 3.

T2 response to hyperoxia*

Maternal hyperoxia had a significant impact on the placental T2* values. The mean placental T2* values rose after oxygenation, and this enhancement was positively correlated to gestational age. This is confirmed by the analysis of the mean T2* ratios (mean $T2^*_{hyperoxia}$/ mean $T2^*_{baseline}$) that were significantly higher in advanced pregnancies than in early ones (Pearson correlation coefficient R = 0.56, 95% CI [0.32, 0.73], p<0.001, Figure 4A). The α and β ratios did not correlate with gestational age: the α ratio ($\alpha_{hyperoxia}$/ $\alpha_{baseline}$) was 1.2 +/- 0.37 and the β ratio ($\beta_{hyperoxia}$/ $\beta_{baseline}$) was 1+/-0.3 (Figure 4C and 4D), suggesting a translation of the histogram towards higher values with a similar overall aspect after hyperoxia.

Functional and dynamic response to hyperoxia

BOLD fitting was successfully performed in 41/52 patients of our cohort, and dynamic parameters were deduced from the sigmoid model fitted to the data, as illustrated in Figure 1C. Two patients were excluded for clinical discomfort. Two others (with uncomplicated pregnancies and normal perinatal outcome) were considered as outliers and excluded from the regression analysis (Figures S2 and S3). In seven other patients, the fitting could not be performed correctly due to contractions or fetal motion close to the placenta, leading to signal changes that could not be controlled for. Overall, 41 cases were included in the BOLD statistical analysis.

The $\Delta BOLD$ (Percentage of BOLD signal enhancement) was positively and significantly related to gestational age. After multiple testing, we finally used a spline regression of degree 2 with a single knot at 24 weeks. This resulted in a slow increase in $\Delta BOLD$ before 24 weeks, followed by a faster increase around 24-26 weeks of gestation (Figure 5A). Conversely, the $\lambda\,(min^{-1})$ parameter, appeared to be negatively (although weakly) correlated to gestational age (Pearson correlation coefficient R = -0.33, 95% CI [-0.58, -0.02], p=0.04, R^2 = 0.1, Figure 5B).

As a combination of both previous parameters, Vmax (% of enhancement.min^{-1}, eq.2), also positively correlated with gestational age (Figure 5C). Hence, the changes in the maximal rate of signal enhancement during oxygen supply throughout gestation were more influenced by the variations of $\Delta BOLD$(%) across gestation than λ (min^{-1}).

DISCUSSION

Assessment of placental functional capacity is challenging. MRI T2*-weighted sequences along with the response to maternal hyperoxia show interesting potential in assessing placental function. Our histogram analysis of the T2* values in normoxia showed a whole-placenta variation, with a decreasing linear trend in both mean T2* signal and α, and a fixed β parameter throughout gestation. While the T2* enhancement correlated with gestational age, both α and β ratios remained stable, suggesting higher T2* values with a similar histogram aspect. The $\Delta BOLD$ showed a non-linear increase across gestation. Conversely, the $\lambda\ (min^{-1})$ parameter, showed an inverted and weaker correlation with gestation. As a combination of $\Delta BOLD$ and λ, variations in Vmax throughout gestation were mainly influenced by the changes in $\Delta BOLD$ and resulted in a positive correlation with gestational age.

The mean placental T2* value was the first MRI biomarker suggested to be of clinical interest for evaluation of placental maturation or dysfunction [15,17,21,26] and was recently evaluated by Hansen et. al as a biomarker of placental dysfunction in a cohort of small-for-gestational-age fetuses with normal Doppler patterns [19]. The results showed a lower predictive performance, suggesting that the global overview of the placental function assessed only by the mean T2* value may not be sufficient.

The decrease in the α parameter across gestation, describing a wider distribution of T2* values in early pregnancies and a progressively sharpening peak, is consistent with previous reports and suggests a change in either placental tissue structure (villous maturations) or functional properties and oxygen levels [13,22]. Indeed, the aging placenta is quite different in tissue maturation and structure than the earlier placenta and fetal interaction with oxygen requirements is also different. These effects will influence the T2* in a non-linear way (based on local differences in susceptibility): maternal blood flow is higher, and the distribution of oxygen through the mature placental tissue will likely be quite different.

Hence, T2* analysis in baseline conditions alone is insufficient to disentangle these effects: comparing baseline to hyperoxia placental histograms appeared essential to evaluate the placental function.

The intensity of placental response to maternal hyperoxia varied according to gestational age. Interestingly, we observed a stability of the other histogram parameter ratios, with both α and β ratios remaining close to 1. Altogether, this suggests a translation of the T2* histogram toward higher values (i.e. a right-shift of the histogram with a similar shape) once the placenta reaches its maximal oxygen uptake capacity, and similar enhancement of all placental areas regardless of gestational age. This goes against the idea of placental non-functioning lobules with advancing gestation and aging placenta.

The effect of gestational age on fetal oxygen levels is well known [27]. As the placental growth slows after the second trimester, fetal growth accelerates, increasing its needs and consumption in nutrients and oxygen to maintain adequate development. This increasing mismatch leads to a drop in fetal oxygen saturation with gestation [20,28]. Our BOLD protocol and subsequent results may be indicative of this mismatch and consistent with a simple free-diffusion model of oxygenation, as suggested by previous reports [24,25]. As maternal arterial blood-pool oxygen saturation is already high, oxygen supply increases PaO_2 (dissolved O_2 in arterial blood pools) rather than SpO_2, which, theoretically, should not modify the signal. Hence, if we consider a free-diffusion model where, as stated by the first Fick's law, $J(t) = -D * \frac{d[O2]}{dt}$, then the increased gradient between maternal and fetal compartments causes an increased oxygen transfer from the mother to the fetus. Therefore, the $\Delta BOLD$ should reflect the difference in oxygen saturations between fetal and maternal compartments (i.e. the signal increase in both fetal and maternal venous blood), and the λ (min^{-1}) parameter should be related to the ability of O_2 to diffuse across the placental interface. Finally, as a combination of both previous parameters, Vmax may be a potential parameter describing the speed of oxygen transfer, depending on both permeability to oxygen diffusion (placental structure) and the difference in oxygen saturations.

$\Delta BOLD$ exhibited a slow increase before 24 weeks, followed by a faster increase, quite similar to the fetal weight-estimation curves [29]. While a similar correlation was found between $\Delta BOLD$ and fetal weight estimation, we found no correlation between the EFW percentile and $\Delta BOLD$ (Figure S4, supplementary material), suggesting that the interpatient variability in fetal weight is not related to placental function.

Overall, our BOLD analysis, constitutes a first step towards the analysis of placental oxygen diffusivity, which may be interesting to differentiate constitutionally small fetuses from intrauterine growth restriction.

Limitations

Several limitations are to be acknowledged. First, our methodology did not allow us to deduce oxygen levels and we could not separate fetal from maternal compartment either with our acquisition or segmentation method. The choice of lying patients in supine position could be debated, as it is known to affect in-utero placental blood flow and oxygen transfer to the fetus, particularly in advanced pregnancies [30–32]. Hence, while the trends of $\Delta BOLD$ across gestation may not be affected, caution should be taken when comparing the raw data with other studies.

A further limitation relies in fitting imprecisions of dynamic parameters in the BOLD protocol. First, in early pregnancies, the placental enhancement is close to the intrinsic signal variability. Along with important fetal motion close to the placenta, this reduces the accuracy of fitting. Second, in case of advanced pregnancies (after 34-35 weeks), the main factor responsible for fitting failure was recurrent contractions during the acquisition, known to induce a reduction in the T2* value with a slow recovery[33].

Conclusion

Our results suggest that the reduction in the T2* signal and apparent placental oxygenation, does not reflect a loss in placental ability to uptake and transfer oxygen to the fetus. Our BOLD results are

consistent with a free-diffusion model of oxygenation, highlighting the growing differences in oxygen saturation between mother and fetus throughout gestation ($\Delta BOLD$), and changes in placental permeability to oxygen (λ), on which depends the speed of oxygen transfer to the fetus. Further studies are needed to evaluate the interest of combined information from static and dynamic measurement of T2* changes, and their ability to determine the remaining placental capacity or identify potential histological lesions.

Conflicts of interest: none

Funding: none

References

1. Avni R, Golani O, Akselrod-Ballin A, Cohen Y, Biton I, Garbow JR, Neeman M. MR Imaging–derived Oxygen-Hemoglobin Dissociation Curves and Fetal-Placental Oxygen-Hemoglobin Affinities. Radiology. 2016;280(1):68-77.

2. Sun C, Groom KM, Oyston C, Chamley LW, Clark AR, James JL. The placenta in fetal growth restriction: What is going wrong? Placenta. 2020;96:10-18. d

3. Lees C, Marlow N, Arabin B, Bilardo CM, Brezinka C, Derks JB, Duvekot J, Frusca T, Diemert A, Ferrazzi E, Ganzevoort W, Hecher K, Martinelli P, Ostermayer E, Papageorghiou AT, Schlembach D, Schneider KTM, Thilaganathan B, Todros T, Van Wassenaer-Leemhuis A, Valcamonico A, Visser GHA, Wolf H, Scheepers HCJ, Spaanderman M, Calvert S, Missfelder-Lobos H, Van Eyck J, Oepkes D, Fratelli N, Prefumo F, Napolitano R, Chaoui R, Maso G, Ogge G, Oberto M, Mensing Van Charante N. Perinatal morbidity and mortality in early-onset fetal growth restriction: Cohort outcomes of the trial of randomized umbilical and fetal flow in Europe (TRUFFLE). Ultrasound Obstet Gynecol. 2013;42(4):400-408.

4. von Beckerath AK, Kollmann M, Rotky-Fast C, Karpf E, Lang U, Klaritsch P. Perinatal complications and long-term neurodevelopmental outcome of infants with intrauterine growth restriction. Am J Obstet Gynecol. 2013;208(2):130.e1-130.e6.

5. Lees CC, Marlow N, Van Wassenaer-Leemhuis A, Arabin B, Bilardo CM, Brezinka C, Calvert S, Derks JB, Diemert A, Duvekot JJ, Ferrazzi E, Frusca T, Ganzevoort W, Hecher K, Martinelli P, Ostermayer E, Papageorghiou AT, Schlembach D, Schneider KTM, Thilaganathan B, Todros T, Valcamonico A, Visser GHA, Wolf H, Aktas A, Borgione S, Chaoui R, Cornette JMJ, Diehl T, Van Eyck J, Fratelli N, Van Haastert IL, Lobmaier S, Lopriore E, Missfelder-Lobos H, Mansi G, Martelli P, Maso G, Maurer-Fellbaum U, Van Charante NM, De Tollenaer SM, Napolitano R, Oberto M, Oepkes D, Ogge G, Van Der Post J, Prefumo F, Preston L, Raimondi F, Reiss IKM, Scheepers HCJ, Schuit E, Skabar A, Spaanderman M, Weisglas-Kuperus N, Zimmermann A, Moore T, Johnson S, Rigano S. 2 year neurodevelopmental and

intermediate perinatal outcomes in infants with very preterm fetal growth restriction (TRUFFLE): A randomised trial. The Lancet. 2015;385(9983):2162-2172.

6. Jaddoe VWV, de Jonge LL, Hofman A, Franco OH, Steegers EAP, Gaillard R. First trimester fetal growth restriction and cardiovascular risk factors in school age children: population based cohort study. BMJ. 2014;348(jan23 1):g14-g14.

7. Sovio U, White IR, Dacey A, Pasupathy D, Smith GCS. Screening for fetal growth restriction with universal third trimester ultrasonography in nulliparous women in the Pregnancy Outcome Prediction (POP) study: A prospective cohort study. The Lancet. 2015;386(10008):2089-2097.

8. Salomon LJ, Alfirevic Z, Da Silva Costa F, Deter RL, Figueras F, Ghi T, Glanc P, Khalil A, Lee W, Napolitano R, Papageorghiou A, Sotiriadis A, Stirnemann J, Toi A, Yeo G. ISUOG Practice Guidelines: ultrasound assessment of fetal biometry and growth. Ultrasound Obstet Gynecol. 2019;53(6):715-723.

9. Bhide A, Acharya G, Baschat A, Bilardo CM, Brezinka C, Cafici D, Ebbing C, Hernandez-Andrade E, Kalache K, Kingdom J, Kiserud T, Kumar S, Lee W, Lees C, Leung KY, Malinger G, Mari G, Prefumo F, Sepulveda W, Trudinger B. ISUOG Practice Guidelines (updated): use of Doppler velocimetry in obstetrics. Ultrasound Obstet Gynecol. 2021;58(2):331-339.

10. Drukker L, Staines-Urias E, Villar J, Barros FC, Carvalho M, Munim S, McGready R, Nosten F, Berkley JA, Norris SA, Uauy R, Kennedy SH, Papageorghiou AT. International gestational age-specific centiles for umbilical artery Doppler indices: a longitudinal prospective cohort study of the INTERGROWTH-21st Project. Am J Obstet Gynecol. 2020;222(6):602.e1-602.e15.

11. Parra-Saavedra M, Crovetto F, Triunfo S, Savchev S, Peguero A, Nadal A, Parra G, Gratacos E, Figueras F. Placental findings in late-onset SGA births without Doppler signs of placental insufficiency. Placenta. 2013;34(12):1136-1141.

12. Lewkowitz AK, Tuuli MG, Cahill AG, Macones GA, Dicke JM. Perinatal outcomes after intrauterine growth restriction and intermittently elevated umbilical artery Doppler. Am J Obstet Gynecol MFM. 2019;1(1):64-73.

13. Hutter J, Jackson L, Ho A, Pietsch M, Story L, Chappell LC, Hajnal JV, Rutherford M. T2* relaxometry to characterize normal placental development over gestation in-vivo at 3T. Wellcome Open Res. 2019;4:166.

14. Sørensen A, Hutter J, Seed M, Grant PE, Gowland P. T2*-weighted placental MRI: basic research tool or emerging clinical test for placental dysfunction? Ultrasound Obstet Gynecol. 2020;55(3):293-302.

15. Sinding M, Sørensen A, Hansen DN, Peters DA, Frøkjær JB, Petersen AC. T2* weighted placental MRI in relation to placental histology and birth weight. Placenta. 2021;114:52-55.

16. Chavhan GB, Babyn PS, Thomas B, Shroff MM, Haacke EM. Principles, Techniques, and Applications of T2*-based MR Imaging and Its Special Applications. RadioGraphics. 2009;29(5):1433-1449.

17. Sinding M, Peters DA, Frøkjær JB, Christiansen OB, Petersen A, Uldbjerg N, Sørensen A. Prediction of low birth weight: Comparison of placental T2* estimated by MRI and uterine artery pulsatility index. Placenta. 2017;49:48-54.

18. Ho AEP, Hutter J, Jackson LH, Seed PT, Mccabe L, Al-Adnani M, Marnerides A, George S, Story L, Hajnal JV, Rutherford MA, Chappell LC. T2* Placental Magnetic Resonance Imaging in Preterm Preeclampsia: An Observational Cohort Study. Hypertens Dallas Tex 1979. 2020;75(6):1523-1531.

19. Hansen DN, Sinding M, Petersen A, Christiansen OB, Uldbjerg N, Peters DA, Frøkjær JB, Sørensen A. T2*-weighted placental magnetic resonance imaging: a biomarker of placental dysfunction in small-for-gestational-age pregnancies. Am J Obstet Gynecol MFM. 2022;4(3):100578.

20. Aughwane R, Mufti N, Flouri D, Maksym K, Spencer R, Sokolska M, Kendall G, Atkinson D, Bainbridge A, Deprest J, Vercauteren T, Ourselin S, David A, Melbourne A. Magnetic resonance imaging measurement of placental perfusion and oxygen saturation in early-onset fetal growth restriction. BJOG Int J Obstet Gynaecol. 2021;128(2):337-345.

21. Poulsen SS, Sinding M, Hansen DN, Peters DA, Frøkjær JB, Sørensen A. Placental T2* estimated by magnetic resonance imaging and fetal weight estimated by ultrasound in the prediction of birthweight differences in dichorionic twin pairs. Placenta. 2019;78:18-22.

22. Steinweg JK, Hui GTY, Pietsch M, Ho A, van Poppel MPM, Lloyd D, Colford K, Simpson JM, Razavi R, Pushparajah K, Rutherford M, Hutter J. T2* placental MRI in pregnancies complicated with fetal congenital heart disease. Placenta. 2021;108:23-31.

23. Schabel MC, Roberts VHJ, Gibbins KJ, Rincon M, Gaffney JE, Streblow AD, Wright AM, Lo JO, Park B, Kroenke CD, Szczotka K, Blue NR, Page JM, Harvey K, Varner MW, Silver RM, Frias AE. Quantitative longitudinal T2* mapping for assessing placental function and association with adverse pregnancy outcomes across gestation. Stevenson GN, ed. PLOS ONE. 2022;17(7):e0270360.

24. Sørensen A, Sinding M, Peters DA, Petersen A, Frøkjaer JB, Christiansen OB, Uldbjerg N. Placental oxygen transport estimated by the hyperoxic placental BOLD MRI response. Physiol Rep. 2015;3(10):e12582.

25. Sinding M, Peters DA, Poulsen SS, Frøkjær JB, Christiansen OB, Petersen A, Uldbjerg N, Sørensen A. Placental baseline conditions modulate the hyperoxic BOLD-MRI response. Placenta. 2018;61:17-23.

26. Pietsch M, Ho A, Bardanzellu A, Zeidan AMA, Chappell LC, Hajnal JV, Rutherford M, Hutter J. APPLAUSE: Automatic Prediction of PLAcental health via U-net Segmentation and statistical Evaluation. Med Image Anal. 2021;72:102145.

27. Soothill PW, Nicolaides KH, Rodeck CH, Campbell S. Effect of Gestational Age on Fetal and Intervillous Blood Gas and Acid-Base Values in Human Pregnancy. Fetal Diagn Ther. 1986;1(4):168-175.

28. Melbourne A, Aughwane R, Sokolska M, Owen D, Kendall G, Flouri D, Bainbridge A, Atkinson D, Deprest J, Vercauteren T, David A, Ourselin S. Separating fetal and maternal placenta circulations using multiparametric MRI. Magn Reson Med. 2019;81(1):350-361.

29. Stirnemann J, Villar J, Salomon LJ, Ohuma E, Ruyan P, Altman DG, Nosten F, Craik R, Munim S, Cheikh Ismail L, Barros FC, Lambert A, Norris S, Carvalho M, Jaffer YA, Noble JA, Bertino E, Gravett MG, Purwar M, Victora CG, Uauy R, Bhutta Z, Kennedy S, Papageorghiou AT, for the International Fetal and Newborn Growth Consortium for the 21st Century (INTERGROWTH-21st), Scientific Advisory Committee, Steering Committees, INTERGROWTH-21st, INTERBIO-21st, Executive Committee, In addition for INTERBIO 21st, Project Coordinating Unit, Data Analysis Group, Data Management Group, In addition for INTERBIO 21st, Ultrasound Group, In addition for INTERBIO-21st:, Anthropometry Group, In addition for INTERBIO-21st:, Laboratory Processing Group, Neonatal Group, Environmental Health Group, Neurodevelopment Group, Participating countries and local investigators, In addition for INTERBIO-21st:, In addition for INTERBIO-21st: International estimated fetal weight standards of the INTERGROWTH-21 st Project: International estimated fetal weight standards. Ultrasound Obstet Gynecol. 2017;49(4):478-486.

30. Abaci Turk E, Abulnaga SM, Luo J, Stout JN, Feldman HA, Turk A, Gagoski B, Wald LL, Adalsteinsson E, Roberts DJ, Bibbo C, Robinson JN, Golland P, Grant PE, Barth WH. Placental MRI: Effect of maternal position and uterine contractions on placental BOLD MRI measurements. Placenta. 2020;95:69-77.

31. Couper S, Clark A, Thompson JMD, Flouri D, Aughwane R, David AL, Melbourne A, Mirjalili A, Stone PR. The effects of maternal position, in late gestation pregnancy, on placental blood flow and oxygenation: an MRI study. J Physiol. 2021;599(6):1901-1915.

32. Jani D, Clark A, Couper S, Thompson JMD, David AL, Melbourne A, Mirjalili A, Lydon A, Stone PR. The effect of maternal position on placental blood flow and fetoplacental oxygenation in late gestation fetal growth restriction: a magnetic resonance imaging study. J Physiol. 2023;601(23):5391-5411.

33. Abaci Turk E, Stout JN, Feldman HA, Gagoski B, Zhou C, Tamen R, Manhard MK, Adalsteinsson E, Roberts DJ, Golland P, Grant PE, Barth WH. Change in T2* measurements of placenta and fetal organs during Braxton Hicks contractions. Placenta. 2022;128:69-71.

FIGURE LEGENDS

Figure 1: Illustration of our MRI protocol. Figure 1A summarizes the overall placental MRI protocol. After a first T2* relaxometry and mapping, a dynamic acquisition was performed, followed by a second T2* relaxometry after oxygen supply); Figure 1B illustrates a T2* relaxometry in a placenta at 29 weeks of gestation along with their corresponding histograms. Left image, placental T2* relaxometry in standard conditions; Right image, same placenta after oxygen saturation. Blue and red histograms correspond to the distribution of T2* values within the placental segmentation before and after oxygen supply, respectively; Figure 1C and 1D illustrates the BOLD effect in five pregnancies at different gestational ages, with normalized signal-over-time curves (blue lines) and corresponding sigmoid fitting (orange line) used to determine the dynamic parameters. Abbreviations: VOI (volume of interest); BOLD (blood oxygen level dependent)

Figure 2: Histogram parameters at baseline. Histogram parameters at baseline, determined from the histogram distribution of placental T2* values. (A) Mean placental T2* signal; (B) minimum T2* values; (C) Placental histogram shape parameter (α); (D) Rate parameter (β). Lower and upper dashed lines represent the 10^{th} and 90^{th} predicted percentiles, respectively.

Figure 3: Simulated changes in placental T2* histogram. The changes in placental T2* histogram across gestation were simulated using the results of figure 2 and modelled using a gamma distribution. As we did not observe a correlation between the rate parameter (β) and gestational, we set its value at 0.12 (mean β in our cohort). Values of the α parameter were generated from the regression equation (23.6-0.42*weeks, figure 2C). This illustrates the change in the overall histogram aspect across gestation, with a diminution of the mean T2* signal, along with increasing homogeneity and right-tailed extension.

Figure 4: T2* response to hyperoxia. Effect of hyperoxia on T2* histogram parameters throughout gestation. The signal enhancement significantly increases with gestational age, as assessed by the mean ratio (A) (Mean $T2^*_{hyperoxia}$/Mean $T2^*_{baseline}$) and the ratio of minimum T2* values (B). The changes in α (C) and β (D) ratios were small and did not correlate with gestational age. Lower and upper dashed lines represent the 10^{th} and 90^{th} predicted percentiles, respectively.

Figure 5: BOLD Functional parameters. Changes in BOLD parameters across gestation. Parameters $\Delta BOLD$ (5A) and λ (5B) were deduced from the sigmoid model. Vmax (5C) describes the maximal steepness, and results from a combination of both parameters. Lower and upper dashed lines represent the 10^{th} and 90^{th} percentiles, respectively. Red dots: 2 cases identified as outliers in the regression model.

Table 1 : Summary of parameters from both acquisitions

PARAMETERS	T2* MAPPING	BOLD
Sequence	ME-GE	GE-EPI
TE [ms]	16 TE (3.0 to 77.3 ms)	Single shot (50ms)
TR [ms]	92.7 ms	8000 ms
FA	30°	90°
FOV [mm]	360 x 360	360 x 360
MATRIX	256 x 256	128 x 128
In-plane resolution [mm]	1.41 x 1.41 mm	2.81 x 2.81 mm
Slice thickness [mm]	7 mm	6 mm
Orientation	Axial	Axial
Breath	Breath hold	Free breathing
Coverage	2-4 slices	8-15 slices
Timepoints	-	75-90

Abbreviations: TE, echo times; TR, repetition time; FA, flip angle; FOV, field of view.

Table 2 : Population characteristics at MRI scan

Prenatal characteristics, N = 52			
Maternal characteristics		**Ultrasound features**	
Age (years)	33 (30.8, 35)	EFW-percentile	50 (39, 69)
Nulliparous	26 (50%)	AC-percentile	62 (44, 75)
BMI	21.40 (20.45, 23)	MCA-PSV (MoM)	1.06 (0.96, 1.18)
First trimester PE risk estimation*	1/548 (1/1368, 1/230)	Uterine artery bilateral notch	1 (1.9%)
Aspirin	5 (9.8%)	Positive umbilical diastole	52 (100%)
Gestational age at MRI scan (weeks)	26.9 (23.3, 32.2)	Positive Ductus venosus A wave	52 (100%)

Abbreviations: BMI, Body mass index; PE, pre-eclampsia; EFW, estimated fetal weight; AC, abdominal circumference; MCA-PSV, middle cerebral artery-peak systolic velocity;

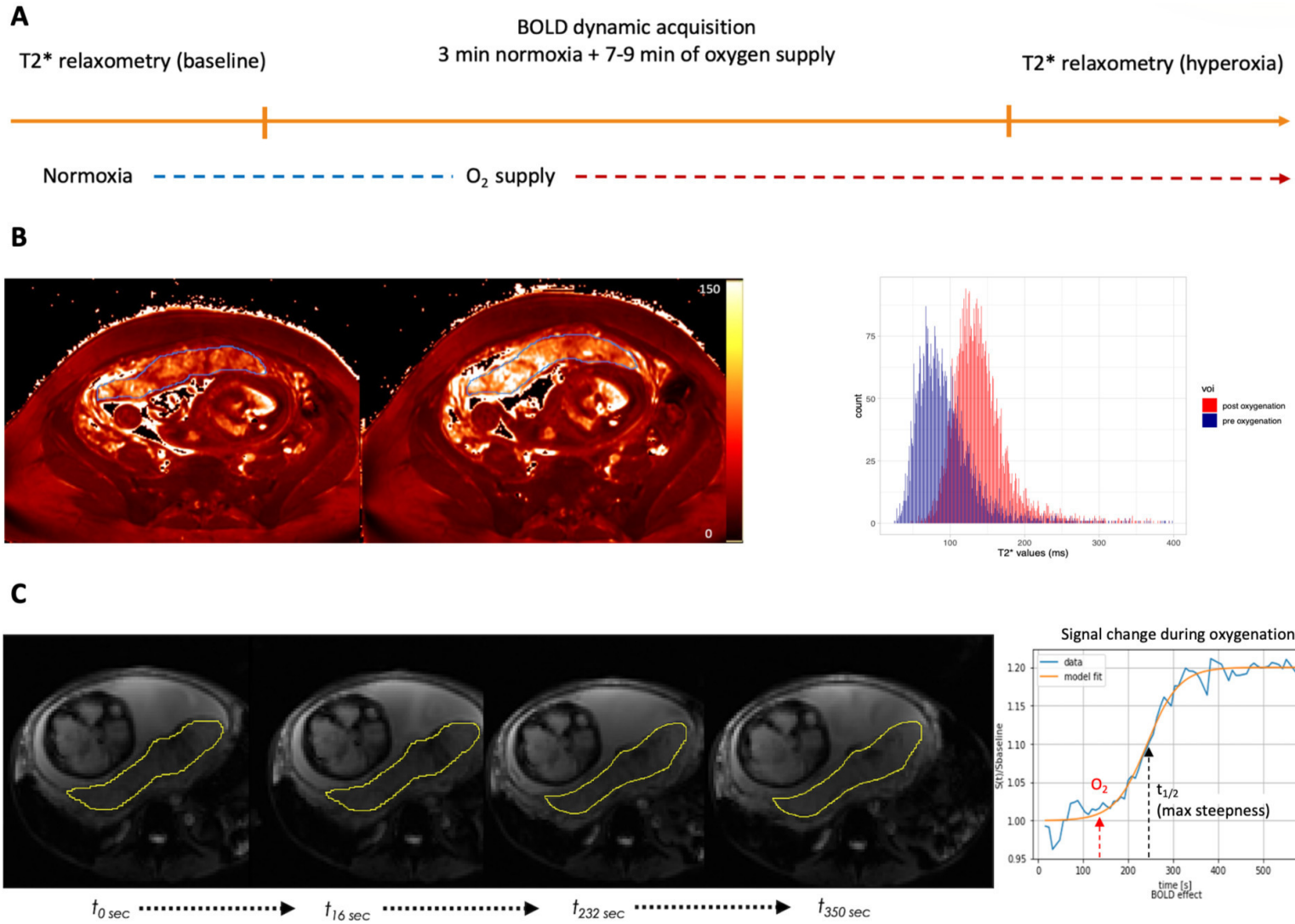

figure 1.jpg

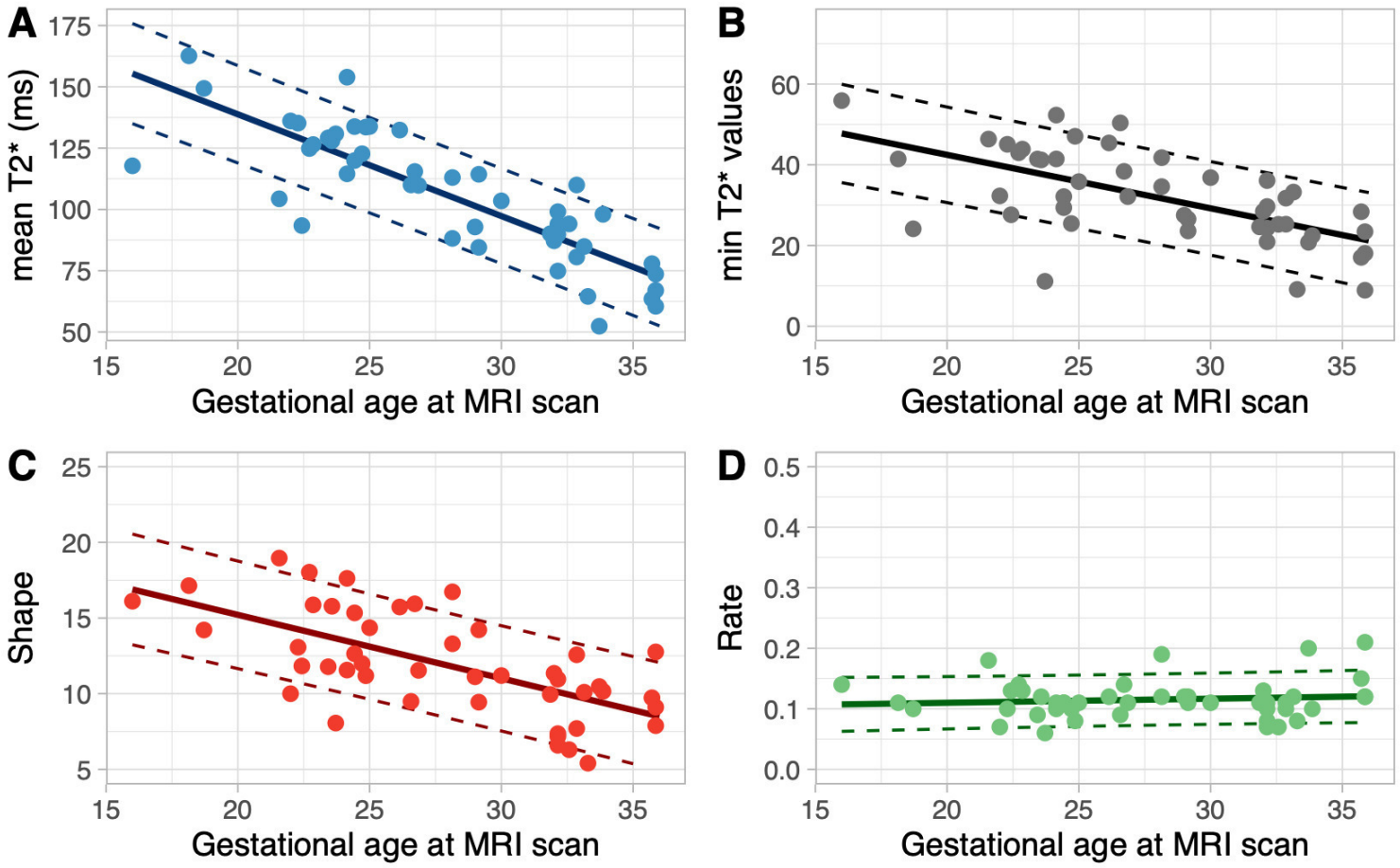

figure 2.jpg

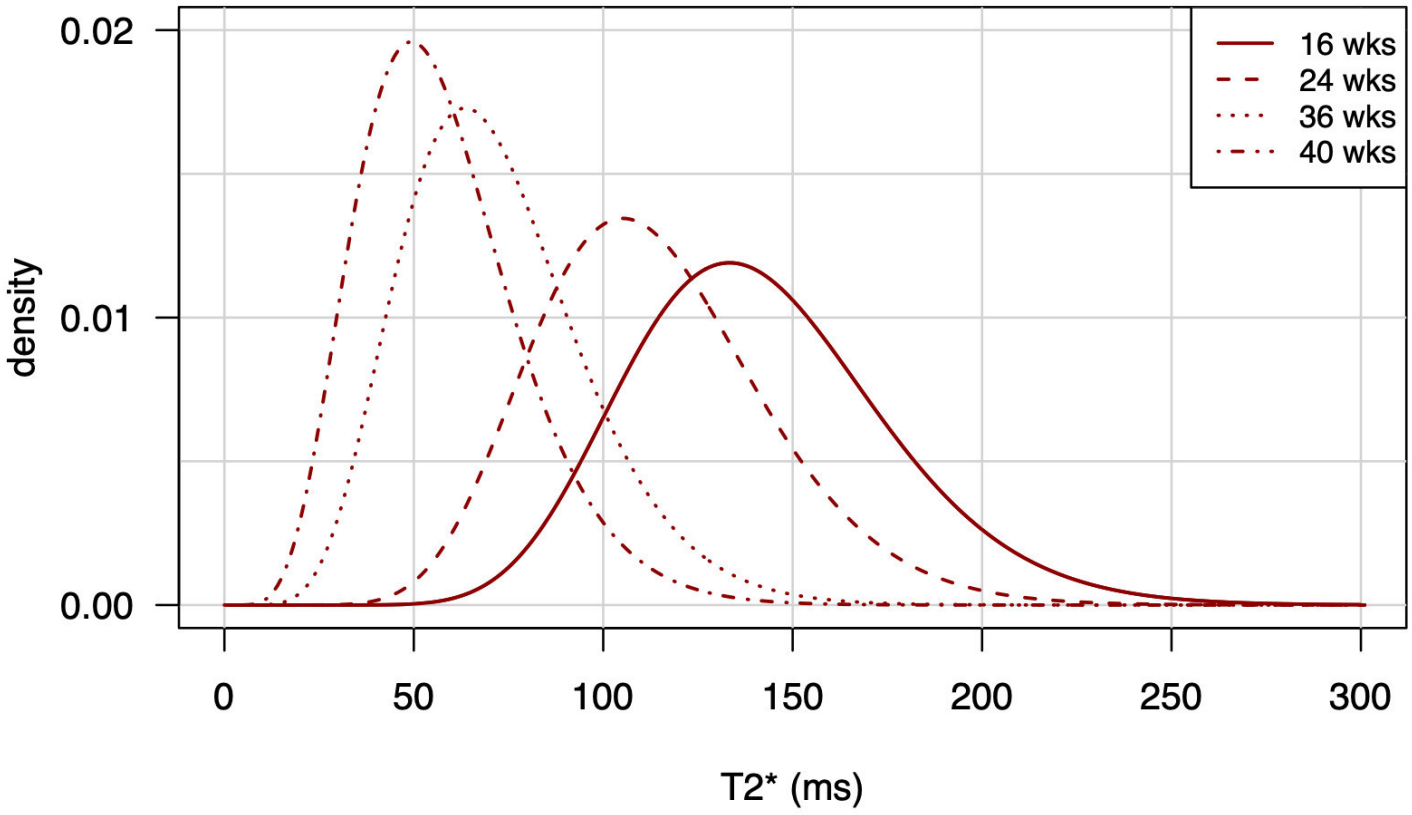

Figure 3.jpg

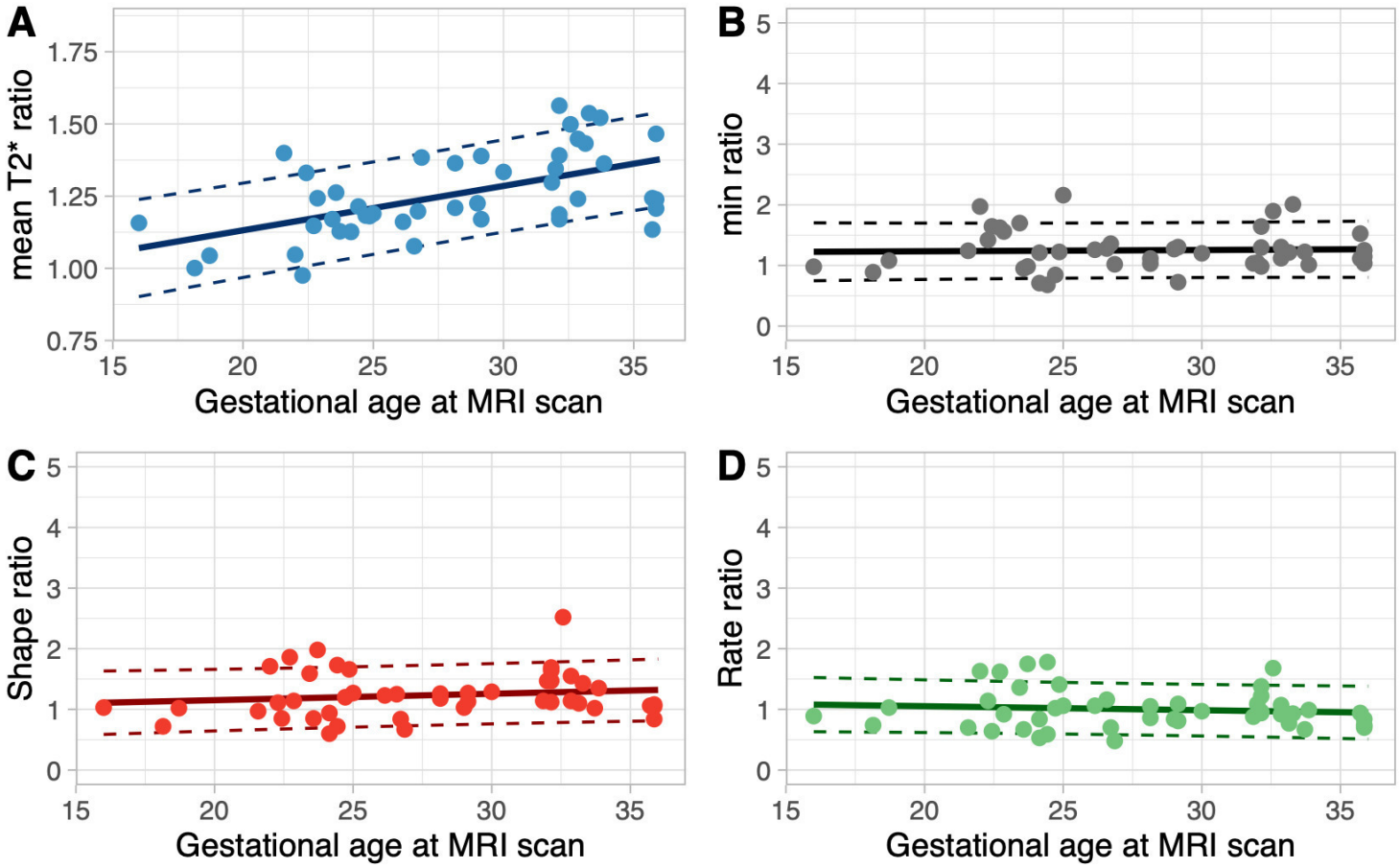

figure 4.jpg

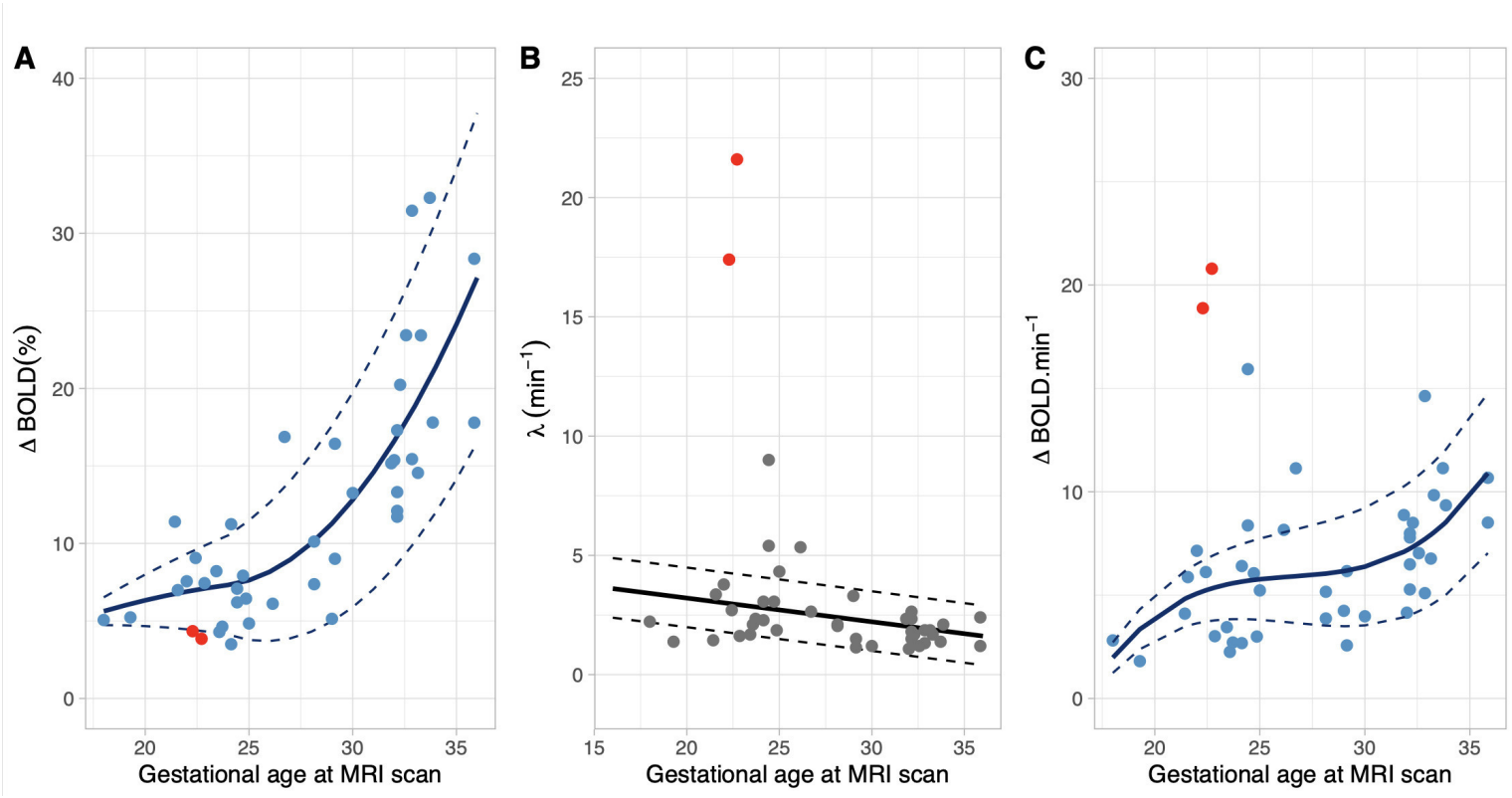

fig5_out.jpg